



## Synthesis and Characterization of Toothpaste Formulated with Nano-hydroxyapatite and Silver Nanoparticles

Fastabiquil K. Rhamdiyah, Sari E. Cahyaningrum\*, Rudiana Agustini

Department of Chemistry, Faculty of Mathematics and Natural Sciences, Universitas Negeri Surabaya. Jl. Ketintang, Gayungan, Surabaya 60231, East Java, Indonesia

## ARTICLE INFO

## ABSTRACT

## Article history:

Received 12 December 2023

Revised 13 January 2024

Accepted 9 August 2024

Published online 01 September 2024

**Copyright:** © 2024 Rhamdiyah *et al.* This is an open-access article distributed under the terms of the [Creative Commons Attribution License](https://creativecommons.org/licenses/by/4.0/), which permits unrestricted use, distribution, and reproduction in any medium, provided the original author and source are credited.

Dental caries is a multifactorial chronic dental disease impacting individuals across various ages. Several studies have shown that cariogenic bacteria primarily cause this disease in the oral cavity, notably *Streptococcus mutans*. Thus, this study aimed to characterize and develop toothpaste formulations by incorporating nano-hydroxyapatite (nHA) and silver nanoparticles (AgNPs) as active agents. The physicochemical properties of different formulations (F0-F5) were assessed, including odour, colour, taste, texture, consistency, homogeneity, pH, spreadability, and foaming ability. The antibacterial activity of the products obtained against *Streptococcus mutans* was tested using varying nHA concentrations (0.75, 1, and 1.25%). The results showed that the toothpaste formulation containing 1% nHA showed the most significant inhibitory effect, leading to an inhibition zone of 15.58 mm in diameter. Based on these findings, toothpaste containing nHA and AgNPs as active constituents was safe and efficacious in preventing dental caries.

**Keywords:** Dental caries, Nano-hydroxyapatite, Silver nanoparticles, Toothpaste.

## Introduction

Dental caries, also known as cavities, is a prevalent dental and oral disease that poses a potential threat to individuals across all age groups, particularly children.<sup>1</sup> Furthermore, this condition is characterized by persistent infections that induce the degradation of a tooth's hard tissues, including enamel, dentin, and cementum.<sup>2</sup> Several studies have shown that dental caries is typically caused by a complex interplay of various factors, including cariogenic bacteria, the host's oral structures (including teeth and saliva), and dietary carbohydrate ingestion.<sup>3</sup> The primary cariogenic bacterium in the oral cavity is *Streptococcus mutans*, which can metabolize carbohydrates into lactic acid.<sup>4</sup> This metabolic process typically reduces salivary pH to critical levels ( $\leq 5.5$ ),<sup>5</sup> thereby triggering the dissolution of minerals in the enamel.<sup>6</sup> A practical method for preventing this condition comprises the systematic control of plaque by consistently brushing teeth using toothpaste formulated with fluoride as a key ingredient.<sup>7</sup> Fluoride in toothpaste is considered the gold standard or benchmark due to its well-documented efficacy in preventing tooth caries.<sup>8</sup> Nevertheless, there are many constraints linked to its application, such as reduced effectiveness in certain circumstances with a pH of  $\leq 4.5$ , the need for calcium ( $\text{Ca}^{2+}$ ) and phosphate ( $\text{PO}_4^{3-}$ ) ions from saliva are requisite for fluoride to manifest preventive effects and high doses are required for optimal outcome.<sup>9,10</sup> Furthermore, continuous and excessive use of fluoride-containing toothpaste, along with the potential risk of ingestion, has been linked to a spectrum of health complications, such as dental and skeletal fluorosis, compromised organ function, and impaired thyroid and endocrine system functionality.

Instead, calcium phosphate-based treatments have emerged as a viable alternative for dental caries prevention and remineralization purposes.<sup>11-14</sup>

Hydroxyapatite ( $\text{Ca}_{10}(\text{PO}_4)_6(\text{OH})_2$ ) is widely recognized as the most thermodynamically stable form of calcium phosphate crystal.<sup>15</sup> This increased stability makes it exceptionally suitable for biomimetic materials due to its high bioactivity and biocompatibility.<sup>16</sup> Furthermore, these properties can be attributed to its chemical structure and morphology, resembling the enamel.<sup>17</sup> Hydroxyapatite (HA) exhibits non-toxic properties, ensuring safety even in cases of ingestion,<sup>18</sup> and functions as a remineralizing agent by elevating the oral pH to a neutral state and supplying calcium ( $\text{Ca}^{2+}$ ) and phosphate ( $\text{PO}_4^{3-}$ ) ions within the demineralization zone.<sup>14,19</sup> Geeta *et al.* (2020) stated that including 1% HA in toothpaste could enhance remineralisation. An elevation in oral pH levels could be attributed to a decrease in the population of cariogenic bacteria, specifically *Streptococcus mutans*.<sup>21</sup> Compared to fluoride, which has a restricted capacity for remineralising the outer layer of the tooth, nano-hydroxyapatite (nHA) particles can fill in microscopic cavities on the enamel surface and penetrate deeper layers of dental lesions.<sup>22-25</sup> Moreover, it has been observed that HA can impede the attachment of bacterial plaque to the enamel surface.<sup>10,26</sup> HA has also been identified as an abrasive substance that can effectively whiten the tooth without causing adverse effects.<sup>27</sup> Several studies have also shown that it can alleviate tooth hypersensitivity by forming a protective barrier over the dentin tubules.<sup>28</sup> At the nanoscale, HA crystals resemble natural apatite enamel crystals and manifest heightened efficacy in controlling biofilms.<sup>26</sup> Despite the extensive use of HA, its antibacterial activity in toothpaste has been reported to be relatively low.<sup>29</sup> This challenge can be addressed by incorporating silver nanoparticles (AgNPs) to increase activity.<sup>30</sup> According to a study by Yin *et al.* (2020), AgNPs show a significant antibacterial effect, particularly against *Streptococcus mutans*. The small size of the AgNPs facilitates their swift penetration into bacterial cells, allowing them to interact with the diverse cellular components and cause cell death.<sup>32</sup> AgNPs are known to infiltrate the demineralised area and form precipitates to enhance the hardness and strength of tooth enamel when faced with acid-induced deterioration.<sup>33</sup> Therefore, this study aimed to characterize and develop a toothpaste formulation by incorporating AgNPs and nHA at concentrations of 0.75, 1, and 1.25% and evaluate

\*Corresponding author. E mail: [saricahyaningrum@unesa.ac.id](mailto:saricahyaningrum@unesa.ac.id)  
Tel: +62-812-3290-484

**Citation:** Rhamdiyah, FK, Cahyaningrum, SE, Agustini, R. Synthesis and Characterization of Toothpaste Formulated with Nano-hydroxyapatite and Silver Nanoparticles. Trop J Nat Prod Res. 2024; 8(8):7970-7978. <https://doi.org/10.26538/tjnpr/v8i8.6>

Official Journal of Natural Product Research Group, Faculty of Pharmacy, University of Benin, Benin City, Nigeria.

their influence on the physicochemical properties and antibacterial effectiveness against *Streptococcus mutans*.

## Materials and Methods

### Chemicals

The chemicals used in this study included beef bone (Wonokromo Traditional Market, Surabaya, Indonesia), distilled water with pH 7 (Botanica Asri Lp., Indonesia), demineralized water (Water One, Onemed Ltd., Indonesia), H<sub>2</sub>O<sub>2</sub> (Globalindo Mega Jaya Ltd., Indonesia), AgNO<sub>3</sub> (99.98%, Merck Ltd., Germany), Na-CMC (Wealthy, Changsu Wealthy and Technology Co., Ltd., China), Sorbitol 70% (Subur Kimia Jaya Lp., Indonesia), Na-benzoate (PuroxS Grains, Emerald Kalama Chemical Llc., Holland), propylene glycol (Buana Chem Lp., Indonesia), Peppermint oil (Naturalpedia Lp., Indonesia), CaCO<sub>3</sub> (Unicarb<sup>®</sup>, Niraku Jaya Abadi Ltd., Indonesia), and coco betaine mild surfactant (Heppi Austin Lp., Indonesia).

### Equipment

The equipment consisted of a pH meter (ATC 2011), FTIR (PerkinElmer Spectrum Two), PSA (BIOBASE BK-802N), XRD (X'pert PRO PANalytical), SEM (HITACHI FLEXSEM 100), and NMR (JEOL JNM-ECS400).

### Plant collection and preparation

Fresh *Carica papaya* leaves were obtained from Surabaya City (Indonesia) in June 2023.

### Preparation of *Carica papaya* aqueous extract

The *papaya* leaves were rinsed thoroughly with flowing and distilled water before being sliced into smaller pieces. The sliced pieces (20 g) were mixed with 100 mL of distilled water in a 200 mL beaker. Furthermore, the mixture was heated to 90°C for 20 minutes and cooled to room temperature. The sample was chilled and filtered using Whatman No. 1 filter paper, and the filtrate was transferred to an opaque container and kept at a temperature of 4°C for further use.<sup>34, 35</sup>

### Preparation of nano-hydroxyapatite (nHA)

The beef bones were fragmented and rinsed with distilled water. The samples were then boiled for 6 hours to remove any remaining fat. After boiling, the specimen was washed with distilled water and immersed in a hydrogen peroxide (H<sub>2</sub>O<sub>2</sub>) solution for 5 hours. Subsequently, the specimen was rinsed with demineralized water and air-dried in sunlight, followed by mass measurement and calcination at 900°C for 6 hours.<sup>36</sup>

### Preparation of *Carica papaya* aqueous extract

The *papaya* leaves were rinsed thoroughly with flowing and distilled water before being sliced into smaller pieces. The sliced pieces (20 g) were mixed with 100 mL of distilled water in a 200 mL beaker. Furthermore, the mixture was heated to 90°C for 20 minutes and cooled to room temperature. The sample was chilled and filtered using Whatman No. 1 filter paper, and the filtrate was transferred to an opaque container and kept at a temperature of 4°C for further use.<sup>35, 36</sup>

### Green synthesis of silver nanoparticles

A mixture of 1 mL of *papaya* leaf water extract and 9 mL of a 1 mM AgNO<sub>3</sub> solution was prepared. The mixture was then heated at 60°C for 20 minutes, and a colour change from yellow to brownish-yellow indicated the formation of silver nanoparticles (AgNPs).<sup>34, 35</sup>

### Characterization of nano-hydroxyapatite and silver nanoparticles gel by FTIR

The vibrational bands of bonds and functional groups in nano-hydroxyapatite (nHA) and silver nanoparticles (AgNPs) were analyzed using Fourier Transformed Infrared Spectroscopy (FTIR) in the wave number range of 4000-400 cm<sup>-1</sup>, using the PerkinElmer Spectrum Two.<sup>36, 37</sup>

### Characterization of nano-hydroxyapatite and silver nanoparticles by particle size analyzer

The particle size of nHA and AgNPs was determined using dynamic light scattering (DLS) with a BIOBASE BK-802 N instrument based on

the Brownian motion principle. In this method, smaller particles had faster speed, while bigger particles moved more slowly.<sup>38, 39</sup>

### Characterization of nano-hydroxyapatite and silver nanoparticles by XRD analysis

The crystal structure and phase purity of nHA were determined by X-ray diffraction (X'pert PRO PANalytical) within a 2θ range spanning 20° to 80°.<sup>40</sup>

### Characterization of nano-hydroxyapatite and silver nanoparticles by SEM analysis

The morphology, including particle structure and surface shape of nHA and AgNPs, was analyzed using scanning electron microscopy (SEM).<sup>41, 42</sup>

### Characterization of nano-hydroxyapatite and silver nanoparticles by <sup>1</sup>H NMR analysis

The characterization of molecules in nHA-AgNPs was analyzed using NMR Spectroscopy (<sup>1</sup>H – NMR, JEOL JNM-ECS400). Furthermore, a total of 10 mg of nHA-AgNPs was dissolved in chloroform and analyzed at 25 °C.<sup>43</sup>

### Preparation of 100 g of toothpaste

The quantity of the ingredients required to prepare 100 g toothpaste is presented in Table 1. In this method, the paste base, sodium carboxymethyl cellulose (Na-CMC), was dispersed in hot water, followed by sodium benzoate previously dissolved in sorbitol. After this step, AgNPs and nHA were added, along with CaCO<sub>3</sub> and peppermint oil. The mixture was then stirred at a constant speed until homogeneity was achieved. Subsequently, coco betaine was added to the mix as a surfactant, and it was stirred gently to avoid excessive foam formation, which could damage the texture of toothpaste.<sup>44</sup>

### Determination of organoleptic properties

Sensory and visual inspections were used to assess the organoleptic parameters (colour, taste, odour, and texture). The toothpaste taste was tested manually, whereas ocular assessment was used for the toothpaste colour. The product's smoothness was further tested by rubbing it between fingertips.<sup>45</sup>

### Determination of homogeneity

Homogeneity testing was performed visually by applying 1 g of toothpaste between two object glasses. A visual examination was conducted to identify the presence of larger granular particles, trapped air bubbles, and colour differences.<sup>46</sup>

### Determination of pH

The pH test consisted of dispersing 1 g of toothpaste in 10 mL distilled water with a pH of 7, and then the mixture pH was measured using a digital pH meter.<sup>47</sup>

### Determination of spreadability

The spreadability was evaluated by applying 0.5 g of toothpaste on a scatter glass, then adding a load weighing 200 g and letting the mixture stand for 1 minute. Furthermore, the diameter of the resulting spread was measured.

### Determination of foaming ability

The foaming ability was determined by adding 1 g of toothpaste and 10 mL of distilled water to a 25 mL measuring cylinder for evaluation. The solution was agitated for 120 seconds at 600 rpm, and the foam quantity obtained was measured.

### Antibacterial activity

An *in-vitro* antibacterial study of the formulated toothpaste was performed using the disc diffusion method with Mueller Hinton Agar (MHA) media against the cariogenic bacterial strain *Streptococcus*

*mutans* (ATCC. 35668). *Streptococcus mutans* bacteria were cultured on MHA media and incubated at 37°C for 24 hours. Following McFarland standards, a bacterial suspension was prepared, yielding a  $1.5 \times 10^8$  CFU/mL concentration. The bacteria suspension was uniformly spread onto media plates using a sterile cotton bud.

Subsequently, the disc dipped in the toothpaste was placed into bacterial plates and incubated at 37°C for 24 hours. This was compared to a commercial toothpaste containing HA as a positive control and a base without active agents as a negative control. The zone of inhibition's diameter was measured in millimetres (mm).<sup>48</sup>

**Table 1:** Composition of toothpaste formulation (100 g)

Ingredients	Function	Quantity (% w/w)					
		F0	F1	F2	F3	F4	F5
nHA	Active agent	0	1	0	0.75	1	1.25
AgNPs	Active agent	0	0	5	5	5	5
Na-CMC	Binding agent	1	1	1	1	1	1
Sorbitol 70%	Humectant	15	15	15	15	15	15
Na-benzoate	Preservative	0.5	0.5	0.5	0.5	0.5	0.5
Propylene glycol	Emulsifiers	5	5	5	5	5	5
Peppermint oil	Flavoring agent	1	1	1	1	1	1
CaCO <sub>3</sub>	Abrasive agent	40	40	40	40	40	40
Coco betaine	Foaming agent	1	1	1	1	1	1
Aquadest up to (%)	Solvent	100	100	100	100	100	100

Note: F0 (Base), F1 (nHA), F2 (AgNPs), F3 (0.75% nHA), F4 (1% nHA), F5 (1.25% nHA)

## Results and Discussion

The synthesis of nano-hydroxyapatite (nHA) was achieved through the calcination method, which yielded a product with high crystallinity. The washing and boiling processes of beef bones removed the residual meat and fat present. The immersion of beef bones in hydrogen peroxide (H<sub>2</sub>O<sub>2</sub>) solution changed their colour from yellowish-white to white. Moreover, H<sub>2</sub>O<sub>2</sub> had a dual role in oxidizing surface impurities on bones and removing bacteria that could be attached to them.<sup>34</sup> During the calcination process, the residual water was evaporated as the temperature reached 100°C. At temperatures less than 450°C, oxidation of organic compounds occurred. MgCO<sub>3</sub> decomposition occurred at 540°C, while CaCO<sub>3</sub> was at 750°C. The remaining minerals in the beef bones were observed when the temperature reached 900°C.<sup>49</sup> The synthesis of AgNPs was achieved using the green synthesis method, as shown in Figure 1, because it produced biocompatible AgNPs suitable for clinical use.<sup>50,51</sup> The synthesis of silver nanoparticles using plant extracts is the most adopted method because the plants are widely distributed, readily available, much safer to handle, and more stable.<sup>52</sup> The plant extract used in this study was a water extract made from the *Carica papaya* leaves. Furthermore, the extract contained several secondary metabolites, including phenolics, alkaloids, flavonoids, tannins, saponins, and steroids.<sup>53</sup> These compounds could act as both reducing and stabilizing agents.<sup>54</sup> During the synthesis process, the phytochemical compounds in the aqueous extract from *carica papaya* leaves facilitated the reduction of silver ions (Ag<sup>+</sup>) to nanoparticles (Ag<sup>0</sup>).<sup>55,56</sup> The AgNO<sub>3</sub> precursor solution changed colour to yellow when the extract was added.<sup>57</sup> The change in colour of the solution indicated the formation of AgNPs.<sup>35,36</sup> Phytochemical compounds could maintain the stability of AgNPs and prevent their agglomeration.<sup>38</sup> The FTIR characterization of nano-hydroxyapatite and silver nanoparticle gel results are presented in Figure 2. Figure 2(a) showed that the typical functional groups of nHA were OH, PO<sub>3</sub><sup>4-</sup>, and CO<sub>3</sub><sup>2-</sup>.<sup>58</sup> The peaks centred at 1058.07 cm<sup>-1</sup> corresponded to the stretching vibration of P-O bonds.<sup>59</sup> While a small peak at 1420.80 cm<sup>-1</sup> indicated the presence of carbonate. The peak with the lowest intensity at 3695.08 cm<sup>-1</sup> was attributed to the stretching vibration of O-H groups.<sup>60</sup> The spectra of AgNPs in Figure 2(b) showed that the peaks at 3318.85 cm<sup>-1</sup> corresponded to O-H stretching vibration, indicating the presence of alcohol and phenols.<sup>61</sup> The strong, intense peak observed at 1636.29 cm<sup>-1</sup> corresponded to the presence of C=C stretching cyclic alkene in the extract.<sup>62</sup> Figure 2(c) shows the spectra of nHA and AgNPs. The presence of a small peak at 1058.07 cm<sup>-1</sup> confirmed the P-O functional

groups of nHA, and the peak at 1636.67 cm<sup>-1</sup> showed O-H bending, which confirmed the absorption of water by nHA-AgNPs materials.<sup>63,64</sup> Also, the nano-hydroxyapatite and silver nanoparticles were characterized by a particle size analyzer. The particle size of synthesized nHA and AgNPs, as shown in Table 2, was determined through dynamic light scattering (DLS) based on the Brownian motion of the particles.<sup>39</sup> The results showed that the synthesized nHA and AgNPs had sizes in the nanoscale ranges (1-100 nm).<sup>65</sup> Although these characterization results provided a rough overview of the sizes in the sample, it was important to note that there was a significant variation, as showed by a standard deviation value of 38.935 and a standard error of 22.479.

**Table 2:** Size distribution by number of nHA, AgNPs, and nHA-AgNPs

Material	Size (nm)	Standard Deviation	Standard Error
Nano-hydroxyapatite (nHA)	5.37	-	-
Silver nanoparticles (AgNPs)	31.54	38.935	22.479
nHA-AgNPs	81.97	-	-

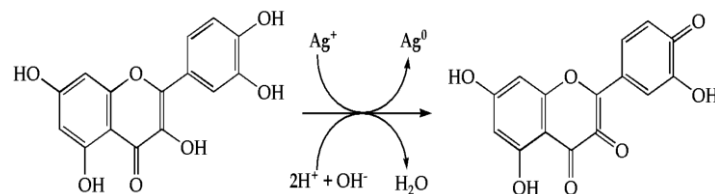


**Figure 1:** Possible reduction mechanisms of Ag<sup>+</sup> ions to AgNPs by flavonols

The synthesized particles were also subjected to characterization using XRD analysis. The nHA was characterized using an X-ray diffraction (XRD) test at the wide angle of  $2\theta = 20$  to  $80^\circ$ , as depicted in Figure 3. The synthesized nHA in Figure 3(a) exhibited similarity to the nHA found in the tissue bank. Furthermore, the product synthesized in Figure

3(a) was predominantly composed of the hydroxyapatite phase, with the highest peak observed at  $2\theta = 31.80^\circ$ , and this was consistent with the JCPDS data number 09-0432.<sup>66</sup> The AKA type (A-type carbonate apatite) with the molecular formula  $\text{Ca}_{10}(\text{PO}_4)_6\text{CO}_3$ , appearing at  $2\theta = 26.02^\circ$  and  $32.27^\circ$ , was formed due to the replacement of  $\text{OH}^-$  ions by  $\text{CO}_3^{2-}$  ions within the nHA structure, with the respective intensities of 40.69 and 63.24%, as indicated by JCPDS data number 35-0180.<sup>29</sup> The AKB type (B-type carbonate apatite) with the molecular formula  $\text{Ca}_{10}(\text{PO}_4)_3(\text{CO}_3)(\text{OH})_2$ , observed at  $2\theta = 28.34^\circ$ , was formed due to the substitution of  $\text{PO}_4^{3-}$  ions by  $\text{CO}_3^{2-}$  ions within the nHA structure, with an intensity of 7.54, as corroborated by JCPDS data number 19-0272.<sup>58</sup> The nano-hydroxyapatite and silver nanoparticles were also characterized by SEM analysis, and the SEM results of nHA are shown in Figure 4(a). The morphology of the nHA powder was characterized by the presence of granular structures of various sizes, which were densely packed close to each other.<sup>67</sup> In Figure 4(b), the SEM results of AgNPs dispersed in a gel base exhibited a smooth surface morphology that seemed to be non-uniform quasi-spherical shapes with clustering tendencies.<sup>68,69</sup>

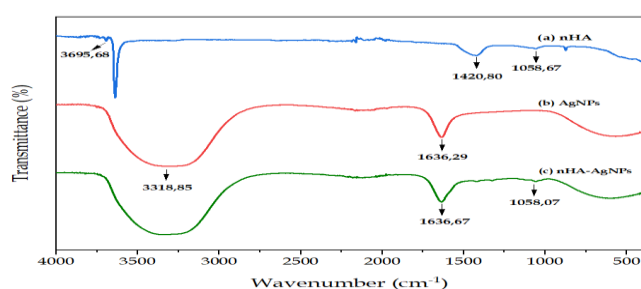


**Figure 2:** FTIR spectra of (a) nano-hydroxyapatite, (b) silver nanoparticles, (c) nHA-AgNPs

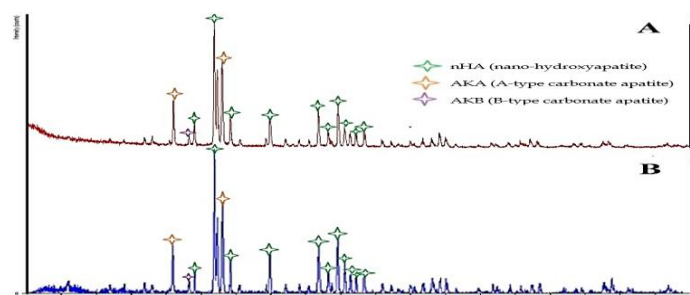


**Figure 3:** XRD patterns of (a) nano-hydroxyapatite from beef bone, (b) nano-hydroxyapatite standard (tissue bank, Dr. Soetomo Hospital).

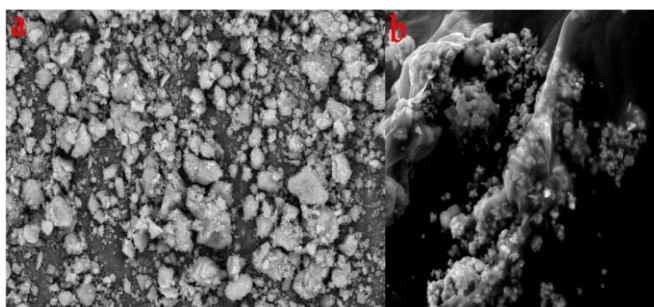


**Figure 4:** SEM image of (a) nano-hydroxyapatite (nHA) from beef bone and (b) silver nanoparticles (AgNPs)

Furthermore, proton NMR ( $^1\text{H}$  NMR) analysis of nHA-AgNPs in chloroform, as presented in Figure 5, provided insights into the molecular characteristics and composition of the sample. A major peak was located at 1.550 ppm with an abundance of 1.5, which could be associated with the organic compounds attaching to the surface of AgNPs or within the nHA matrix. The peak at 2.175 ppm with an

abundance of 0.25 indicated the presence of protons in methylene ( $\text{CH}_2$ ) groups in organic compounds in the composite structure. The presence of a peak at 1.625 ppm with an abundance of 0.2 and a chemical shift similar to the peak at 2.175 ppm could indicate the presence of methyl ( $\text{CH}_3$ ) groups in the sample. This peak could originate from different components or represent variations in the chemical environment of the proton-proton interactions. Several other peaks at 0.842 ppm, 0.825 ppm, and 0.877 ppm with varying abundances could also be associated with water on the apatite surface associated with protons in methyl or methylene groups. Meanwhile, the peaks at 3.733 ppm, 3.717 ppm, and 3.698 ppm, with varying levels of abundance, indicated the presence of protons from water molecules. This suggested that the samples contained water-soluble constituents in chloroform, which could be important information in the context of the application of nHA-AgNPs, particularly in medical or biomedical use.<sup>43,70,71</sup>

The combination of nano-hydroxyapatite and silver nanoparticles toothpaste was also evaluated. Sodium carboxymethyl cellulose (Na-CMC) was a hydrogel binder for gel formation, water absorption, and preventing phase separation between powdered and liquid components. This led to the creation of toothpaste that maintained a consistently smooth and stable texture during storage. Furthermore, sorbitol served as a humectant in toothpaste, preserving its moisture and providing a sweet taste without negative impacts on dental health.<sup>72</sup> Na-benzoate was a preservative used in toothpaste to prevent bacterial growth and maintain its quality during production, storage, and use.<sup>73</sup> Propylene glycol acted as an emulsifier, helping to stabilize ingredients that did not readily dissolve in each other and providing a pleasant taste. Peppermint oil was an aromatic substance that provided a cooling and refreshing sensation when applied. Calcium carbonate ( $\text{CaCO}_3$ ) was an abrasive substance used for removing stains and plaque from the tooth, while coco betaine was a natural surfactant for foaming agents.<sup>72-77</sup> The results of the sensory and physical assessments of the toothpaste, as shown in Table 3, indicated that all formulations had the same attributes regarding odour, colour, taste, texture, and consistency. This study suggested that the specific types of nHA and AgNPs used in toothpaste did not affect its sensory properties. Using the right amount of binder could create a soft texture, reducing the chance of gum injury. The toothpaste's semi-solid texture provided a pleasurable sensation when applied. Abrasiveness is the ability of toothpaste to clean the tooth without causing damage to the enamel.<sup>78,79</sup> Homogeneity is widely recognised as a significant indicator of toothpaste quality. It indicates that all constituent elements had been uniformly dispersed and blended within the base, which served as the dispersion medium. This characteristic ensured the achievement of the highest possible therapeutic efficacy while minimizing the potential for irritation to the oral mucosa upon application.<sup>80</sup> pH is a crucial factor in toothpaste formulation, and the test results showed that the level was below 10.5, indicating that it was safe for oral use and would not cause irritation to the oral mucosa.<sup>81</sup> Using products with a low pH could irritate and encourage the growth of cariogenic bacteria, particularly *Streptococcus mutans*. Alkaline toothpaste could neutralize acidity in the mouth, preventing bacterial growth. Excessive alkalinity often causes dryness of the oral mucosa or the appearance of scale-like formations.<sup>82</sup> The pH test results showed that higher concentrations of nHA in the formulation led to increased pH levels.

Spreadability measures how effectively toothpaste can distribute and cover the teeth, gums, and surrounding areas during application.<sup>47</sup> This parameter is a key characteristic of toothpaste that affects how effectively it delivers active ingredients to the desired area in the right amount. Furthermore, it affected the ease of application, spread on the teeth, and consumer acceptance.<sup>83</sup>

The addition of surfactants, such as coco betaine or other similar substances, influenced the foam production of toothpaste. Surfactants could reduce surface tension, emulsify lipids, and create foam, which helped to remove oral plaque, debris, and food particles. Toothpaste with high foaming capacity is likely to promote better dental hygiene.<sup>47</sup> The antibacterial activity results of the formulated toothpaste in Table 4 indicated that all toothpaste formulations exhibited significant antibacterial effects against *Streptococcus mutans*, the predominant microorganism associated with dental caries within the oral cavity.<sup>84</sup>

The outcomes suggested that incorporating nHA and AgNPs as active ingredients in toothpaste formulation exhibited antibacterial properties against *Streptococcus mutans*. Sample F4, which contained 1% nHA, had the most significant antibacterial activity, as evidenced by an inhibition zone of 15.58 mm (Figure 6). Jariyawattanachaiikul *et al.* (2016) stated that a clear zone with a diameter range of 15-19 mm was included in the very sensitive category in inhibiting bacterial growth.<sup>85</sup>

The antibacterial activity of the formulated toothpaste was due to nHA and AgNPs as the active ingredients.<sup>86</sup> The small size of AgNPs allowed them to penetrate bacterial cells quickly and interact with various cellular components, thereby causing bacterial death.<sup>32</sup> In toothpaste formulation, hydroxyapatite could bind to microorganisms within the mouth by interacting with bacterial adhesins, leading to the microbes' agglutination and subsequent removal from the oral cavity.<sup>28</sup>

**Table 3:** Physicochemical characteristics of toothpaste

Test Parameters	Formulation					
	F0	F1	F2	F3	F4	F5
Odor	Mint	Mint	Mint	Mint	Mint	Mint
Colour	White	White	White	White	White	white
Taste	Fresh	Fresh	Fresh	Fresh	Fresh	Fresh
Texture	Soft	Soft	Soft	Soft	Soft	Soft
Consistency	Semi solid	Semi solid	Semi solid	Semi solid	Semi solid	Semi solid
Homogeneity	Good	Good	Good	Good	Good	Good
pH	8.3	9.47	8.71	9.02	9.29	9.37
Spreadability (cm)	6.3	5.8	6.2	6	5.9	5.7
Foamability (mL)	16	18	16	19	20	20
Abrasiveness	Good	Good	Good	Good	Good	Good

Note: F0 (Base), F1 (nHA), F2 (AgNPs), F3 (0.75% nHA), F4 (1% nHA), F5 (1.25% nHA)

**Table 4:** Antibacterial activity of toothpaste formulation

Formulation	Zone of inhibition (mm)			Average	Category
	1	2	3		
F0 (negative control)	0	0	0	0	Not sensitive
F1	10.02	10.04	10.06	10.04	Sensitive
F2	11.07	11.03	11.05	11.05	Sensitive
F3	14.85	14.9	14.89	14.88	Sensitive
F4	15.57	15.61	15.56	15.58	Very sensitive
F5	13.52	13.51	13.47	13.50	Sensitive
F6 (positive control)	19.33	19.3	19.36	19.33	Very sensitive

Note: F0 (Base), F1 (nHA), F2 (AgNPs), F3 (0.75% nHA), F4 (1% nHA), F5 (1.25% nHA), F6 (Positive control, commercial toothpaste)

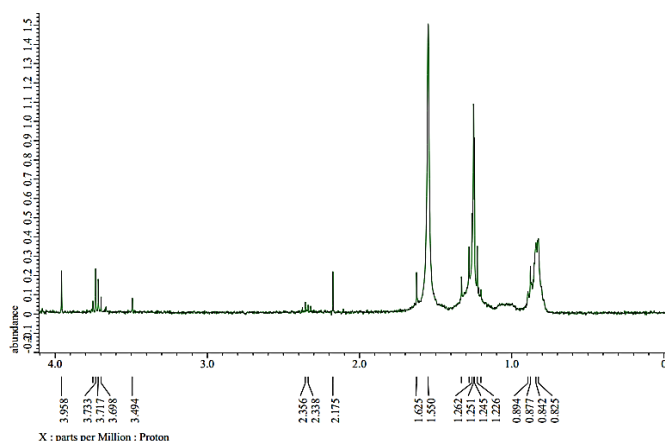


**Figure 5:** <sup>1</sup>H NMR spectra of nHA-AgNPs

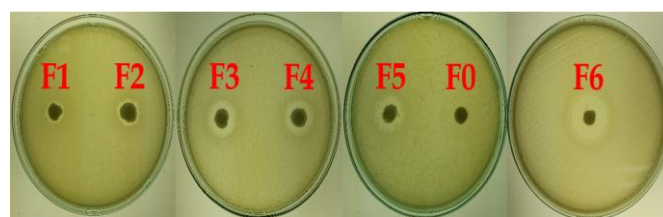


**Figure 6:** Zone of inhibition test for antibacterial activity of F1 (nHA), F2 (AgNPs), F3(0.75% nHA), F4 (1% nHA), F5 (1.25% nHA), F0 (base or negative control), F6 (positive control)

## Conclusion

This study showed that toothpaste formulated with a combination of nano-hydroxyapatite (nHA) and silver nanoparticles (AgNPs) possess good physicochemical characteristics and are safe to use. Furthermore, adding nHA and AgNPs as active ingredients has been shown to increase oral hygiene maintenance and prevent dental caries by inhibiting the growth of cariogenic bacteria *Streptococcus mutans*. The toothpaste formulation containing 1% nHA showed the most substantial inhibitory effect against the test organism, with an inhibition zone of 15.58 mm in diameter, categorized as sensitive.

## Conflict of Interest

The authors declare no conflict of interest.

## Authors' Declaration

The authors hereby declare that the work presented in this article is original and that any liability for claims relating to the content of this article will be borne by them.

## Acknowledgments

The authors are grateful to DRTPM (Direktorat Riset, Teknologi, dan Pengabdian Kepada Masyarakat) for funding this study through a master's thesis research scheme with contract number 145/E5/PG/02.00.PL/2023 dated 19<sup>th</sup> June 2023.

## References

- Bramantoro T, Setijanto RD, Palupi R, Aghazy AZ, Irmalia WR. Dental Caries and Associated Factors among Primary School Children in Metropolitan City with the Largest Javanese Race Population: A Cross-sectional Study. *Contemp Clin Dent*. 2019; 10(2): 274-283. doi: [10.4103/ccd.ccd\\_517\\_18](https://doi.org/10.4103/ccd.ccd_517_18).
- Tinanoff, N. 12 - Dental caries. (6<sup>th</sup> ed.). Online: Elsevier Inc.; 2019. 169-179 p.
- Chen X, Daliri EB-M, Kim N, Kim J-R, Yoo D, Oh D-H. Microbial Etiology and Prevention of Dental Caries: Exploiting Natural Products to Inhibit Cariogenic Biofilms. *Pathogens*. 2020; 9(7): 1–15. doi: [10.3390/pathogens9070569](https://doi.org/10.3390/pathogens9070569).
- Lemos JA, Palmer SR, Zeng L, Wen ZT, Kajfasz JK, Freires IA, Abranches K, Brady LJ. The Biology of *Streptococcus mutans*. *Microbiol Spectr*. 2019; 7(1): 1-26. doi: [10.1128/microbiolspec.GPP3-0051-2018](https://doi.org/10.1128/microbiolspec.GPP3-0051-2018).
- Damian L-R, Dumitrescu R, Alexa VT, Focht D, Schwartz C, Balean O, Jumance D, Obistoiu D, Lalescu D, Stefaniga S-A, Berbecea A, Fratila AD, Scurtu AD, Galuscan A. Impact of Dentistry Materials on Chemical Remineralisation/Infiltration versus Salivary Remineralisation of Enamel-*In Vitro* Study. *Materials (Basel)*. 2022; 15(20): 7258.
- Shahzad HB, Awais F, Shirazi U-e-R, Majeed HA, Rafique A, Shahbaz M. The impact of dental caries on oral health related quality of life amongst adult population in Lahore, Pakistan. *Makara J Heal Res*. 2020; 24(1): 1-7. doi: [10.7454/msk.v24i1.1074](https://doi.org/10.7454/msk.v24i1.1074).
- Lorenz K, Hoffmann T, Heumann C, Noack B. Effect of toothpaste containing amine fluoride and stannous chloride on the reduction of dental plaque and gingival inflammation. A randomized controlled 12-week home-use study. *Int J of Dent Hyg*. 2019; 17(3): 237-243. doi: [10.7454/msk.v24i1.1074](https://doi.org/10.7454/msk.v24i1.1074).
- Paul CC, Khan MAS, Sarkar PK, Hakim A, Waliullah M, Mandal BH. Assessment of the Level and Health Risk of Fluoride and Heavy Metals in Commercial Toothpastes in Bangladesh. *Indones J Chem*. 2020; 20(1):150-159. doi: [10.22146/ijc.43266](https://doi.org/10.22146/ijc.43266).
- Amaechi BT, AbdulAzees PA, Alshareif DO, Shehata MA, Lima PP de CS, Abdollahi A, Kalkhorani PS, Evans V. Comparative efficacy of a hydroxyapatite and a fluoride toothpaste for prevention and remineralization of dental caries in children. *BDJ Open*. 2019; 5(1): 1-15. doi: [10.1038/s41405-019-0026-8](https://doi.org/10.1038/s41405-019-0026-8).
- Meyer F, Enax J, Amaechi BT, Limeback H, Fabritius H-O, Ganss B, Pawinska M, Paszynka E. Hydroxyapatite as Remineralization Agent for Children's Dental Care. *Front Dent Med*. 2022; 3: 1-10. doi: [10.3389/fdmed.2022.859560](https://doi.org/10.3389/fdmed.2022.859560).
- Mohideen H, Dahiya DS, Parsons D, Hussain H, Ahmed RS. Skeletal Fluorosis: A Case of Inhalant Abuse Leading to a Diagnosis of Colon Cancer. *J Investig Med High Impact Case Rep*. 2022; 10.
- Wang Y, Jiang L, Zhao Y. Awareness of the Benefits and Risks Related to Using Fluoridated Toothpaste Among Doctors: A Population-Based Study. *Med Sci Monit*. 2019; 25: 6397-6404.
- Han J, Kiss L, Mei H, Remete AM, Ponikvar-Svet M, Sedgwick DM, Roman R, Fustero S, Moriwaki H, Soloshonok VA. Chemical Aspects of Human and Environmental Overload with Fluorine. *Chem Rev*. 2021; 121(8): 4678-4742. doi: [10.1021/acs.chemrev.0c01263](https://doi.org/10.1021/acs.chemrev.0c01263).
- Anil A, Ibraheem WI, Meshni AA, Preethanath RS, Anil S. Nano-Hydroxyapatite (nHAp) in the Remineralization of Early Dental Caries: A Scoping Review. *Int J Env Res Pub Heal*. 2022; 19(9): 1-14. doi: [10.3390/ijerph19095629](https://doi.org/10.3390/ijerph19095629).
- Ibrahim M, Labaki M, Giraudon J-M, Lamonier J-F. Hydroxyapatite, a multifunctional material for air, water and soil pollution control: A review. *J Hazard Mater*. 2020; 383: 12119. doi: [10.1016/j.jhazmat.2019.121139](https://doi.org/10.1016/j.jhazmat.2019.121139).
- Filip DG, Surdu V-A, Paduraru AV, Andronescu E. Current Development in Biomaterials—Hydroxyapatite and Bioglass for Applications in Biomedical Field: A Review. *J Funct Biomater*. 2022; 13(4) 248. doi: [10.3390/jfb13040248](https://doi.org/10.3390/jfb13040248).
- Imran E, Cooper PR, Ratnayake J, Ekambaram M, Mei ML. Potential Beneficial Effects of Hydroxyapatite Nanoparticles on Caries Lesions *In Vitro*—A Review of the literature. *Dent J (Basel)*. 2023; 11(2):40. doi: [10.3390/dj11020040](https://doi.org/10.3390/dj11020040).
- Hernawan AD, Anggresani L, Meirista I. Formulation of hydroxyapatite toothpaste from mackerel (*Scomberomorus guttatus*) bone waste. *Chempublish J*. 2021; 6(1): 34-45. doi: [10.22437/chp.v6i1.10859](https://doi.org/10.22437/chp.v6i1.10859).
- Rifada A, Af'idah BM, Aufia W, Vibriani A, Maghdalena M, Saputro K, Nugroho, DW, Iskandar MA, Cahyanto A, Noviyanto A, Rochman, NT. Effect of Nano Hydroxyapatite in Toothpaste on Controlling Oral Microbial Viability. *IOP Conf Ser Mater Sci Eng*. 2020; 924(1): 1-7. doi: [10.1088/1757-899X/924/1/012010](https://doi.org/10.1088/1757-899X/924/1/012010).
- Geeta RD, Vallabhaneni S, Fatima K. Comparative evaluation of remineralization potential of nanohydroxyapatite crystals, bioactive glass, casein phosphopeptide-amorphous calcium phosphate, and fluoride on initial enamel lesion (scanning electron microscope analysis) - An *in vitro* study. *J Conserv Dent*. 2020; 23(3): 275-279. doi: [10.4103/JCD.JCD\\_62\\_20](https://doi.org/10.4103/JCD.JCD_62_20).
- Srivastava S, Saha S, Kumari M, Mohd S. Effect of Probiotic Curd on Salivary pH and *Streptococcus mutans*: A Double Blind Parallel Randomized Controlled Trial. *J Clin Diagn Res*. 2016; 10(2):ZC13-6. doi: [10.7860/JCDR/2016/15530.7178](https://doi.org/10.7860/JCDR/2016/15530.7178).
- Amaechi, BT, Lemke, KC, Saha, S, Luong, MN, Gelfond J. Clinical efficacy of nanohydroxyapatite-containing toothpaste at relieving dentin hypersensitivity: an 8 weeks randomized control trial. *BDJ Open*. 2021; 7(1): 1-8. doi: [10.1038/s41405-021-00080-7](https://doi.org/10.1038/s41405-021-00080-7).
- Bordea IR, Candrea S, Alexescu GT, Bran S, Băciuț M, Băciuț G, Lucaciu O, Dinu CM, Todea DA. Nano-hydroxyapatite use in dentistry: a systematic review. *Drug Metab Rev*. 2020; 52(2): 319-332. doi: [10.1080/03602532.2020.1758713](https://doi.org/10.1080/03602532.2020.1758713).
- Gintu AR, Kristiani EBE, Martono Y. Characterization of toothpaste made from abrasive materials hydroxyapatite (HAP). *J Kim Ris*. 2023; 5(2): 120-126. doi: [10.20473/jkr.v5i2.22503](https://doi.org/10.20473/jkr.v5i2.22503).
- Pushpalatha C, Gayathri VS, Sowmya SV, Augustine D, Alamoudi A, Zidane B, Albar NHM, Bhandi S. Nanohydroxyapatite in Dentistry: A comprehensive review. *Saudi Dent J*. 2023; 35(6): 741-752.
- O'Hagan-Wong K, Enax J, Meyer F, Ganss B. The use of hydroxyapatite toothpaste to prevent dental caries.

- Odontology. 2022; 110(2): 223-230. doi: [10.1007/s10266-021-00675-4](https://doi.org/10.1007/s10266-021-00675-4).
27. Sarembe S, Enax J, Morawietz M, Kiesow A, Meyer F. In Vitro Whitening Effect of a Hydroxyapatite-Based Oral Care Gel. *Eur J Dent*. 2020; 14(3): 335-341. doi: [10.1055/s-0040-1714759](https://doi.org/10.1055/s-0040-1714759).
  28. Chen L, Al-Bayatee S, Khurshid Z, Shavandi A, Brunton P, Ratnayake J. Hydroxyapatite in Oral Care Products—A Review. *Materials (Basel)*. 2021; 14(17): 1-20. doi: [10.3390/ma14174865](https://doi.org/10.3390/ma14174865).
  29. Muhaimin FI, Cahyaningrum SE, Lawarti RA, Maharani DK. Characterization and Antibacterial Activity Assessment of Hydroxyapatite-Betel Leaf Extract Formulation against *Streptococcus mutans* *In Vitro* and *In Vivo*. *Indones J Chem*. 2023; 23(2): 358-369. doi: [10.22146/ijc.77853](https://doi.org/10.22146/ijc.77853).
  30. Silva-Holguín PN, Reyes-López SY. Synthesis of Hydroxyapatite-Ag composite as antimicrobial agent. *Dose Response*. 2020; 18(3): 1-14. doi: [10.1177/1559325820951342](https://doi.org/10.1177/1559325820951342).
  31. Yin IX, Zhao IS, Mei ML, Li Q, Yu OY, Chu CH. Use of Silver Nanomaterials for Caries Prevention: A Concise Review. *Int J Nanomedicine*. 2020; 15: 3181-3191. doi: [10.2147/IJN.S253833](https://doi.org/10.2147/IJN.S253833) (2020).
  32. Jinu U, Gomathi M, Saiqa I, Geetha N, Benelli G, Venkatachalam P. Green-engineered biomolecule-capped silver and copper nano-hybrids using *Prosopis cineraria* leaf extract: Enhanced antibacterial activity against microbial pathogens of public health relevance and cytotoxicity on human breast cancer cells (MCF-7). *Microb Pathog*. 2017; 105: 86-95. doi: [10.1016/j.micpath.2017.02.019](https://doi.org/10.1016/j.micpath.2017.02.019).
  33. Pushpalatha C, Bharkhavy KV, Shakir A, Augustine D, Sowmya SV, Bahammam HA, Bahammam SA, Albar NHM, Zidane B. The Anticariogenic Efficacy of Nano Silver Fluoride. *Front Bioeng Biotechnol*. 2022; 10. doi: [10.3389/fbioe.2022.931327](https://doi.org/10.3389/fbioe.2022.931327).
  34. Jalab J, Abdelwahed W, Kitaz A, Al-Kayali R. Green synthesis of silver nanoparticles using aqueous extract of *Acacia cyanophylla* and its antibacterial activity. *Heliyon*. 2021; 7(9): e08033. doi: [10.1016/j.heliyon.2021.e08033](https://doi.org/10.1016/j.heliyon.2021.e08033).
  35. Maarebia RZ, Wahab AW, Taba P. Synthesis and Characterization of Silver Nanoparticles Using Water Extract of Sarang Semut (*Myrmecodia pendans*) for Blood Glucose Sensors. *Indones Chim Acta*. 2019; 12(1):29. doi: [10.20956/ica.v12i1.5881](https://doi.org/10.20956/ica.v12i1.5881).
  36. Afifah F, Cahyaningrum SE. Synthesis and Characterization of Hydroxyapatite from Beef Bone (*Bos taurus*) using Calcination Technique. *Unesa J Chem*. 2020; 9(3): 189-196. doi: [10.26740/ujc.v9n3.p189-196](https://doi.org/10.26740/ujc.v9n3.p189-196).
  37. Nayem ASM, Sultana N, Haque MA, Miah B, Hasan MM, Islam T, Hasan MM, Awal A, Uddin J, Aziz MA, Ahammad AJS. Green Synthesis of Gold and Silver Nanoparticles by using *Amorphophallus paeoniifolius* tuber extract and evaluation of their antibacterial activity. *Molecules*. 2020; 25(20): 1-14. doi: [10.3390/molecules25204773](https://doi.org/10.3390/molecules25204773).
  38. Alslash M, Abdelwahed W, Kitaz A. Green synthesis of silver nanoparticles using *Pistacia palaestina* (Boiss). Extract: Evaluation of *in vivo* wound healing activity. *J Res Pharm*. 2023; 27(3): 1170-1187. doi: [10.29228/jrp.407](https://doi.org/10.29228/jrp.407).
  39. Effendi MC, Pratiwi AR, Afifah F, Taufiq A. The Role of Chicken Egg Shell Nano- Nano-Hydroxyapatite as Fillers on the Surface Hardness of Glass Ionomer Cement. *Malaysian J Fundam Appl Sc*. 2021; 17(4): 475-484. doi: [10.11113/mjfas.v17n4.2192](https://doi.org/10.11113/mjfas.v17n4.2192).
  40. Szcześ A, Hołysz L, Chibowski E. Synthesis of hydroxyapatite for biomedical applications. *Adv Colloid Interface Sci*. 2017; 249: 321-330. doi: [10.1016/j.cis.2017.04.007](https://doi.org/10.1016/j.cis.2017.04.007).
  41. Al-Hamdan RS, Almutairi B, Kattan HF, Alresayes S, Abduljabbar T, Vohra F. Assessment of Hydroxyapatite Nanospheres Incorporated Dentin Adhesive. A SEM/EDX, Micro-Raman, Microtensile and Micro-Indentation Study. *Coatings*. 2020; 10(12): 1181. doi: [10.3390/coatings10121181](https://doi.org/10.3390/coatings10121181).
  42. Jaast S, Grewal A. Green synthesis of silver nanoparticles, characterization and evaluation of their photocatalytic dye degradation activity. *Curr Res Green Sustain Chem*. 2021; 4: 100195. doi: [10.1016/j.crgsc.2021.100195](https://doi.org/10.1016/j.crgsc.2021.100195).
  43. Jing Y, Li J, Zhang Y, Zhang R, Zheng Y, Hu B, Wu L, Zhang D. Structural characterization and biological activities of a novel polysaccharide from *Glehnia littoralis* and its application in preparation of nano-silver. *Int J Biol Macromol*. 2021; 183: 1317-1326. doi: [10.1016/j.ijbiomac.2021.04.178](https://doi.org/10.1016/j.ijbiomac.2021.04.178).
  44. Jagtap AM, Kaulage SR, Kanse SS, Shelke VD, Gavade AS, Vambhurkar GB, Todkar RR, Dange VN. Preparation and Evaluation of Toothpaste. *Asian J Pharm Anal*. 2018; 8(4): 191-194. doi: [10.5958/2231-5675.2018.00035.2](https://doi.org/10.5958/2231-5675.2018.00035.2).
  45. Phalke PL, Rukari TG, Jadhav AS. Formulation and Evaluation of Toothpaste Containing Combination of Aloe and Sodium Chloride. *Int J Pharm Sci Res*. 2019; 10(3): 1462-1467. doi: [10.13040/IJPSR.0975-8232.10](https://doi.org/10.13040/IJPSR.0975-8232.10).
  46. Nuraskin C, Reza R, Salfiyadi T, Abdurrahman A, Faisal TI, Soraya C. Toothpaste Activity Test of Laban Leaf Methanol Extract (*Vitex pinnata*) Against The Growth of *Streptococcus mutans* Bacteria. *Open Access Maced J Med Sci*. 2021; 9(F): 95-100. doi: [10.3889/oamjms.2021.5702](https://doi.org/10.3889/oamjms.2021.5702).
  47. Adeleye OA, Bamiro O, Akpotu M, Adebowale M, Daodu J, Sodeinde MA. Physicochemical Evaluation and Antibacterial Activity of *Massularia acuminata* Herbal Toothpaste. *Turk J Pharm Sci*. 2021; 18(4): 476-482. doi: [10.4274/tjps.galenos.2020.42966](https://doi.org/10.4274/tjps.galenos.2020.42966).
  48. Gautam D, Palkar P, Maule K, Singh S, Sawant G, Kuvalekar C, Rukari T, Jagtap VA. Preparation, Evaluation, and Comparison of Herbal Toothpaste with Marketed Herbal Toothpaste. *Asian J Pharm Technol*. 2020; 10(3): 165-169. doi: [10.5958/2231-5713.2020.00028.8](https://doi.org/10.5958/2231-5713.2020.00028.8).
  49. Lindawati Z, Cahyaningrum, SE. Effect of Hydroxyapatite/Chitosan/Collagen Composition on Bone Graft Characteristics. *Unesa J Chem*. 2018; 7(3): 101-104. doi: [doi.org/10.26740/ujc.v7n3.p%25p](https://doi.org/10.26740/ujc.v7n3.p%25p).
  50. Singh P, Pandit S, Garnæs J, Tunjic S, Mokkapat V, Sultan A, Thygesen A, Mackevia A, Mateiu RV, Daugaard AE, Baun A, Mijakovic I. Green synthesis of gold and silver nanoparticles from *Cannabis sativa* (industrial hemp) and their capacity for biofilm inhibition. *Int J Nanomedicine*. 2018; 13: 3571-3591. doi: [10.2147/IJN.S157958](https://doi.org/10.2147/IJN.S157958).
  51. Simon S, Sibuyi NRS, Fadaka AO, Meyer S, Josephs J, Onani MO, Meyer M, Madiehe AM. Biomedical Applications of Plant Extract-Synthesized Silver Nanoparticles. *Biomedicine*. 2022; 10(11): 2792. doi: [10.3390/biomedicine10112792](https://doi.org/10.3390/biomedicine10112792).
  52. Hossain MR., Biplob AI, Sharif SR, Bhuiya AM, Sayem ASM. Antibacterial Activity of Green Synthesized Silver Nanoparticles of *Lablab purpureus* Flowers Extract against Human Pathogenic Bacteria. *Trop J Nat Prod Res*. 2023; 7(8): 3647-3651. doi: [10.26538/tjpr/v7i8.12](https://doi.org/10.26538/tjpr/v7i8.12).
  53. Singh SP, Kumar S, Mathan S V, Tomar MS, Singh RK, Verma PK, Kumar A, Kumar S, Singh RP, Acharya A. Therapeutic application of *Carica papaya* leaf extract in the management of human diseases. *DARU J Pharm Sci*. 2020; 28(2): 735-44. doi: [10.1007/s40199-020-00348-7](https://doi.org/10.1007/s40199-020-00348-7).
  54. Kuppusamy P, Yusoff MM, Maniam GP, Govindan N. Biosynthesis of metallic nanoparticles using plant derivatives and their new avenues in pharmacological applications – An updated report. *Saudi Pharm J*. 2016; 24(4): 473-484. doi: [10.1016/j.jsps.2014.11.013](https://doi.org/10.1016/j.jsps.2014.11.013).
  55. Arsene MMJ, Viktorovna PI, Alla M, Mariya M, Davares AKL, Carime BZ, Anatolievna GO, Vyacheslavovna YN, Vladimirovna ZA, Andreevna BL, Aleksandrovna VE, Alekseevich BL, Nikolaevna SM, Parfait K, Andrey V. Antimicrobial activity of phytobiosynthesized silver nanoparticles using *carica papaya* L. against Gram-negative

- bacteria. *Vet World*. 2023; 16(6): 1301-1311. doi: [10.14202/vetworld.2023.1301-1311](https://doi.org/10.14202/vetworld.2023.1301-1311).
56. Banala RR, Nagati VB, Karnati PR. Green synthesis and characterization of *Carica papaya* leaf extract coated silver nanoparticles through X-ray diffraction, electron microscopy and evaluation of bactericidal properties. *Saudi J Biol Sci*. 2015; 22(5): 637-644. doi: [10.1016/j.sjbs.2015.01.007](https://doi.org/10.1016/j.sjbs.2015.01.007).
  57. Purnamasari MD, Wijayati N. Antibacterial Synthesis of Silver Nanoparticles using Bioreductor Belt Leaf Extract with Microwave Irradiation. *Indones J Chem Sci*. 2016; 5(2): 152-158.
  58. Cahyaningrum SE, Herdyastuty N, Devina B, Supangat D. Synthesis and Characterization of Hydroxyapatite Powder by Wet Precipitation Method. *IOP Conf Ser Mater Sci Eng*. 2018; 299(1): 1-5. doi: [10.1088/1757-899X/299/1/012039](https://doi.org/10.1088/1757-899X/299/1/012039).
  59. Muñoz-Sanchez ER, Arrieta-Gonzalez CD, Quinto-Hernandez A, Garcia-Hernandez E, Porcayo-Calderon J. Synthesis of hydroxyapatite from eggshell and its electrochemical characterization as a coating on titanium. *Int J Electrochem Sci*. 2023; 18(9): 100204. doi: [10.1016/j.ijeos.2023.100204](https://doi.org/10.1016/j.ijeos.2023.100204).
  60. Kumar KCV, Subha TJ, Ahila KG, Ravindran B, Chang SW, Mahmoud AH, Mohammed OB, Rathi MA. Spectral characterization of hydroxyapatite extracted from Black Sumatra and Fighting cock bone samples: A comparative analysis. *Saudi J Biol Sci*. 2021; 28(1): 840-846. doi: [10.1016/j.sjbs.2020.11.020](https://doi.org/10.1016/j.sjbs.2020.11.020).
  61. Jyoti K, Baunthiyal M, Singh A. Characterization of silver nanoparticles synthesized using *Urtica dioica* Linn. leaves and their synergistic effects with antibiotics. *J Radiat Res Appl Sci*. 2016; 9(3): 217-227. doi: [10.1016/j.jrras.2015.10.002](https://doi.org/10.1016/j.jrras.2015.10.002).
  62. Vijapur LS, Srinivas Y, Desai AR, Gudigenavar AS, Shidramshettar SL, Yaragattimath P. Development of biosynthesized silver nanoparticles from *Cinnamomum tamala* for anti-oxidant, anti-microbial and anti-cancer activity. *J Res Pharm*. 2023; 27(2): 769-782. doi: [10.29228/jrp.359](https://doi.org/10.29228/jrp.359).
  63. Bee S-L, Bustami Y, Ul-Hamid A, Lim K, Hamid ZAA. Synthesis of silver nanoparticle-decorated hydroxyapatite nanocomposite with combined bioactivity and antibacterial properties. *J Mater Sci Mater Med*. 2021; 32(9): 106. DOI: [10.1007/s10856-021-06590-y](https://doi.org/10.1007/s10856-021-06590-y).
  64. Hossain N, Islam MA, Chowdhury MA. Synthesis and characterization of plant-extracted silver nanoparticles and advances in dental implant applications. *Heliyon*. 2022; 8(12): e12313. doi: [10.1016/j.heliyon.2022.e12313](https://doi.org/10.1016/j.heliyon.2022.e12313). Khan I, Saeed K, Khan I. Nanoparticles: Properties, applications and toxicities. *Arab J Chem*. 2017; 12(7): 908-931. doi: [10.1016/j.arabjc.2017.05.011](https://doi.org/10.1016/j.arabjc.2017.05.011).
  65. Hariani PL, Said M, Salni. Effect of sintering on the mechanical properties of hydroxyapatite from fish bone (*Pangasius Hypophthalmus*). *IOP Conf Ser Mater Sci Eng*. 2019; 509: 012109. doi: [10.1088/1757-899X/509/1/012109](https://doi.org/10.1088/1757-899X/509/1/012109).
  66. Jang SJ, Kim SE, Han TS, Son JS, Kang SS, Choi SH. Bone Regeneration of Hydroxyapatite with Granular Form or Porous Scaffold in Canine Alveolar Sockets. *In Vivo (Brooklyn)*. 2017; 31(3): 335-341. doi: [10.21873/invivo.11064](https://doi.org/10.21873/invivo.11064).
  67. Salari Z, Danafar F, Dabaghi S, Ataei SA. Sustainable synthesis of silver nanoparticles using macroalgae *Spirogyra varians* and analysis of their antibacterial activity. *J Saudi Chem Soc*. 2016; 20(4): 459-464. doi: [10.1016/j.jscs.2014.10.004](https://doi.org/10.1016/j.jscs.2014.10.004).
  68. Huang J, Li Q, Sun D, Lu Y, Su Y, Yang X, Wang H, Wang Y, Shao W, He N, Hong J, Chen C. Biosynthesis of silver and gold nanoparticles by novel sundried *Cinnamomum camphora* leaf. *Nanotechnology*. 2007; 18(10): 105104. doi: [10.1088/0957-4484/18/10/105104](https://doi.org/10.1088/0957-4484/18/10/105104).
  69. Byra N, Krukowski S, Sadlo J, Kolodziejki W. Composites Containing Nanohydroxyapatites and a Stable TEMPO Radical: Preparation and Characterization Using Spectrophotometry, EPR and 1H MAS NMR. *Materials (Basel)*. 2022; 15(6): 1-28. doi: [10.3390/ma15062043](https://doi.org/10.3390/ma15062043).
  70. Kavitha C, Dasan KP. Nanosilver/hyperbranched polyester (HBPE): Synthesis, characterization, and antibacterial activity. *J Coatings Technol Res*. 2013; 10(5): 669-678. doi: [10.1007/s11998-013-9499-x](https://doi.org/10.1007/s11998-013-9499-x).
  71. Widyastuti W, Fantari HR, Putri VR, Pertiwi I. Toothpaste formulation of orange (*Citrus sp.*) peel extract and mint leaves (*Mentha Piperita L.*) and activity against *Streptococcus mutans* bacteria. *J Pharmascience*. 2019; 6(2): 111. doi: [10.20527/jps.v6i2.7357](https://doi.org/10.20527/jps.v6i2.7357).
  72. Asrina R. Stabel toothpaste formulation from ethanol extract of Gamal leaves extract (*Gliricida sepium*) to prevent dental caries. *J Farm Sandi Karsa*. 2019; 18(5): 99-104. doi: [10.36060/jfs.v5i2.50](https://doi.org/10.36060/jfs.v5i2.50).
  73. Tabatabaei MH, Mahounak FS, Asgari N, Moradi Z. Cytotoxicity of the Ingredients of Commonly Used Toothpastes and Mouthwashes on Human Gingival Fibroblasts. *Front Dent*. 2020; 16(6):450-457. doi: [10.18502/fid.v16i6.3444](https://doi.org/10.18502/fid.v16i6.3444).
  74. Behra JS, Mattsson J, Cayre OJ, Robles ESJ, Tang H, Hunter TN. Characterization of Sodium Carboxymethyl Cellulose Aqueous Solutions to Support Complex Product Formulation: A Rheology and Light Scattering Study. *ACS Appl Polym Mater*. 2019; 1(3): 344-358. doi: [10.1021/acsapm.8b00110](https://doi.org/10.1021/acsapm.8b00110).
  75. Zhao H, Ren S, Yang H, Tang S, Guo C, Liu M, Tao Q, Ming T, Xu H. Peppermint essential oil: its phytochemistry, biological activity, pharmacological effect and application. *Biomed Pharmacother*. 2022; 154: 113559. doi: [10.1016/j.biopha.2022.113559](https://doi.org/10.1016/j.biopha.2022.113559).
  76. Jannah Z, Mubarak H, Syamsiyah F, H Putri AA, Rohmawati L. Preparation of Calcium Carbonate (from Shellfish)/Magnesium Oxide Composites as an Antibacterial Agent. *IOP Conf Ser Mater Sci Eng*. 2018; 367: 012005. doi: [10.1088/1757-899X/367/1/012005](https://doi.org/10.1088/1757-899X/367/1/012005).
  77. Dionysopoulos D, Papageorgiou S, Papadopoulos C, Davidopoulou S, Konstantinidis A, Tolidis K. Effect of Whitening Toothpastes with Different Active Agents on the Abrasive Wear of Dentin Following Tooth Brushing Simulation. *J Funct Biomater*. 2023; 14(5): 268. doi: [10.3390/jfb14050268](https://doi.org/10.3390/jfb14050268).
  78. Sinaga MH, Bintarti T. The combination of kecombrang flowers (*Etlinger elation* JACK) and banana peels in toothpaste formulations are effective in antibacterial testing against *Streptococcus mutans* and *Escherichia coli*. *J Ilm PANNMED*. 2019; 14(1): 85-90. doi: [10.36911/panmed.v14i1.568](https://doi.org/10.36911/panmed.v14i1.568).
  79. Lini R. Formulation and Physical Properties Test of Gel Toothpaste for Dry Red Ginger (*Zingiber Officinale* Roscoe *Var. Rubrum*) Extract. *J Penelit Farm Indones*. 2021; 10(1): 6-11. doi: [10.51887/jpfi.v10i1.994](https://doi.org/10.51887/jpfi.v10i1.994).
  80. Cheng C-Y, Balsandorj Z, Hao Z, Pan L. High-precision measurement of pH in the full toothpaste using NMR chemical shift. *J Magn Reson*. 2020; 317: 106771. doi: [10.1016/j.jmr.2020.106771](https://doi.org/10.1016/j.jmr.2020.106771).
  81. Hasan M, Solang M, Kumaji SS. Analysis of the number of bacteria in *Anadara granosa* shell toothpaste provided by Citrus Medika with different storage times. *Biospecies*. 2021; 14(1): 46-52.
  82. Riani M, Darusman F, Suparman A. Formulation of toothpaste preparations from Arabic bidara leaf extract (*Ziziphus Spina-Christi L.*). *Pros Farm*. 2020; 1(2): 636-642. doi: [10.29313/V6I2.23556](https://doi.org/10.29313/V6I2.23556).
  83. Dinis M, Agnello M, Cen L, Shokeen B, He X, Shi W, Wong DTW, Lux R, Tran NC. Oral Microbiome: *Streptococcus mutans*/Caries Concordant-Discordant Children. *Front Microbiol*. 2022;13. doi: [10.3389/fmicb.2022.782825](https://doi.org/10.3389/fmicb.2022.782825).



84. Jariyawattanachaikul W, Chaveerach P, Chokesajjawatee N. Antimicrobial Activity of Thai-herbal Plants against Food-borne Pathogens *E. Coli*, *S. Aureus* and *C. jejuni*. *Agric Sci Procedia*. 2016; 11: 20-24. doi: 10.1016/j.aaspro.2016.12.004.
85. Vijayaraghavan P, Rathi MA, Almaary KS, Alkhattaf FS, Elbadawi YB, Chang SW, Ravindran B. Preparation and antibacterial application of hydroxyapatite doped silver nanoparticles derived from chicken bone. *J King Saud Univ - Sci*. 2022; 34(2): 101749. doi: [10.1016/j.jksus.2021.101749](https://doi.org/10.1016/j.jksus.2021.101749).